Journal of the Less-Common Metals, 175 (1991) 143–154
LCM 1254

Magnetic structures of $TbMn_6Sn_6$ and $HoMn_6Sn_6$ compounds from neutron diffraction study

B. Chafik El Idrissi, G. Venturini and B. Malaman
Laboratoire de Chimie du Solide Minéral, Université de Nancy I, associé au CNRS, UA 158, B.P. 239, 54506 Vandoeuvre-les-Nancy Cédex (France)

D. Fruchart
Laboratoire de Cristallographie du CNRS, associé à l'Université J. Fourier, 166X, 38042 Grenoble Cédex (France)

(Received March 13, 1991)

Abstract

Neutron diffraction measurements have been performed on the ternary stannides $TbMn_6Sn_6$ and $HoMn_6Sn_6$ of $HfFe_6Ge_6$ type structure (space group, *P6/mmm*). This structure can be described as a filled derivative of the CoSn B35-type structure. Each of the rare earth and manganese atoms is successively distributed in alternate layers stacked along the *c* axis with the sequence Mn–R–Mn–Mn–R–Mn. Owing to the manganese atom coordination of the rare earth, this structure appears closely related to the $CaCu^5$- and $ThMn_{12}$-type structures. This study confirms that both the rare earth and the manganese sublattices order simultaneously above room temperature. In the whole temperature range studied (2–300 K), $TbMn_6Sn_6$ and $HoMn_6Sn_6$ exhibit a collinear ferrimagnetic arrangement. At 300 K, the magnetic structure consists of a stacking of ferromagnetic (001) layers of rare earth and manganese with the coupling sequence Mn(+)R(−)Mn(+)Mn(+)-R(−)Mn(+) ($\mu_{Mn} \approx 2.0(1)\mu_B$, $\mu_{Tb} = 4.9(1)\mu_B$, $\mu_{Ho} = 4.7(1)\mu_B$). For $HoMn_6Sn_6$, the magnetic moments lie in the (001) plane while in $TbMn_6Sn_6$, they deviate by $\phi = 15°$ from the *c* axis. Below 300 K, the two compounds exhibit a spin rotation process and at 2 K the magnetic moments are along [001] and at 50° from this axis for $TbMn_6Sn_6$ and $HoMn_6Sn_6$ respectively ($\mu_{Mn} = 2.4(1)\mu_B$, $\mu_{Tb} = 8.6(1)\mu_B$, $\mu_{Ho} = 8.4(1)\mu_B$).

The results are discussed in terms of Ruderman–Kittel–Kasuy–Yoshida exchange interactions and compared with those obtained previously for the parent RFe_6Al_6 and RCo_5 compounds.

1. Introduction

In previous papers we reported on the crystallographic data and magnetic properties of new ternary stannides RMn_6Sn_6 (R ≡ Sc, Y, Gd–Tm, Lu) [1, 2]. All these compounds crystallize in the $HfFe_6Ge_6$ type structure [3] which is closely related to the well-known $CaCu_5$- and $ThMn_{12}$-type structures [4]. From this point of view, it was rather interesting to study their magnetic properties.

Magnetic measurements on RMn_6Sn_6 (R ≡ Sc, Y, Gd–Tm, Lu) polycrystalline samples have been largely described in ref. 2. RMn_6Sn_6 compounds (R ≡ Y, Sc, Lu) are characterized by an antiferromagnetic ordering of the

0022-5088/91/$3.50

manganese sublattice ($T_N > 330$ K) while they behave ferromagnetically for some of the rare earth elements (R ≡ Gd–Ho) ($T_C = 423$ K and $T_C = 376$ K for $TbMn_6Sn_6$ and $HoMn_6Sn_6$ respectively). At lower temperatures, some of them (R ≡ Tb, Ho) exhibit an additional magnetic transition ($T_t = 330$ K and $T_t = 200$ K for $TbMn_6Sn_6$ and $HoMn_6Sn_6$ respectively) which could be related to a reorientation of the easy axis from the (001) plane to the *c* axis. Moreover, the magnetic measurements revealed that the rare earth sublattice orders at the same time as the manganese sublattice and the saturation moment values observed for these two compounds ($\mu \approx 3.3\mu_B$ and $\mu = 3.7\mu_B$ for $TbMn_6Sn_6$ and $HoMn_6Sn_6$ respectively) are rather compatible with a ferrimagnetic behaviour due to antiferromagnetic coupling of rare earth and manganese ferromagnetic sublattices. Furthermore, one other interesting property is the occurrence of rather high coercive fields for these compounds which reach more than 11 kOe in $TbMn_6Sn_6$ at 4.2 K.

In this paper, we report on the magnetic structures derived from neutron diffraction experiments of two of these compounds: $TbMn_6Sn_6$ which has the higher coercive field and $HoMn_6Sn_6$ whose second magnetic transition occurs in the studied 2–300 K temperature range.

2. Sample preparation

All the compounds were prepared from commercially available high purity elements: manganese (powder, 99.9%), rare earth elements (ingot, 99.9%) and tin (powder, 99.99%). Pellets of starting composition RMn_6Sn_6 (R ≡ Y, Tb or Ho) were compacted using a steel die, and were annealed several times (with grinding and compacting each time) at 1073 K in sealed silica tubes under argon (0.2 atm) and finally quenched in water. The purity of the final samples was determined by X-ray diffraction using a Guinier camera (Cu Kα). The polycrystalline ingots revealed small single crystals. The best-shaped crystals (R ≡ Tb, Sc) were studied by X-ray diffraction using a four-circle diffractometer (Nonius CAD 4F).

3. Structure determination

The X-ray diffraction patterns obtained from powder samples show that all these compounds are single-phase materials, with the $HfFe_6Ge_6$-type structure. The crystal structure of $HfFe_6Ge_6$ is an ordered filled derivative of the CoSn-B35 type (space group, *P6/mmm*) [1]. This structure can also be described as built of alternate (001) layers containing magnetic rare earth and manganese atoms, respectively. The rare earth atoms occupy hexagonal planes (H) and the manganese atoms form Kagomé nets (K) stacked along the *c* axis with the sequence --KHKKHK-- [2] (Fig. 1). Furthermore, as regards the manganese and rare earth coordination polyhedra around the rare earth (Fig. 1), this structure is closely related to the $CaCu_5$ (*P6/mmm*) and $ThMn_{12}$

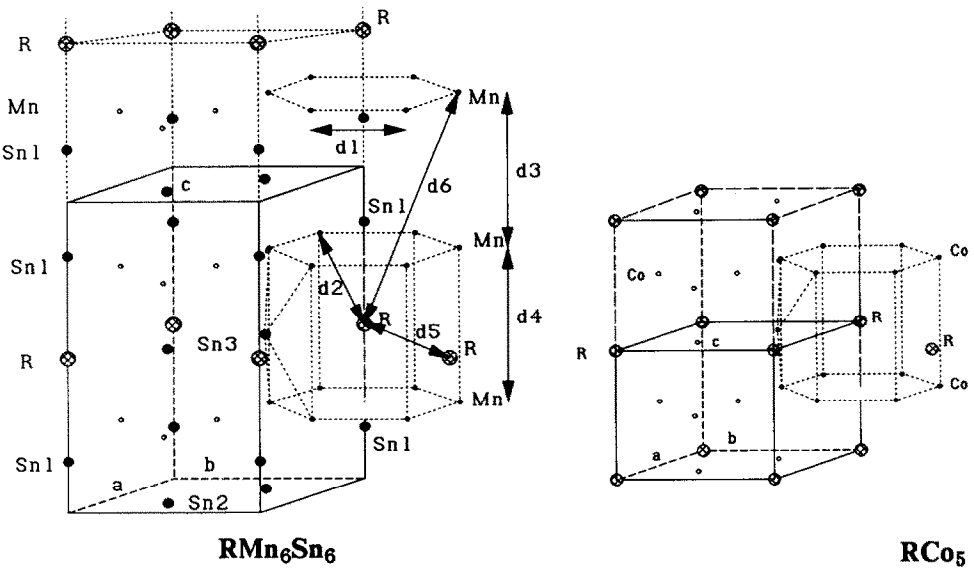

Fig. 1. Structures of RMn_6Sn_6 and $CaCu_5$ showing structural relationships (the distances d_i are related to those indicated in Table 1).

TABLE 1

Atomic positions and thermal parameters of $TbMn_6Sn_6$ [4]

Atom	Position	Symmetry	x	y	z	B (Å^2)
Tb	1(b)	6/*mmm*	0	0	1/2	0.35(3)
Mn	6(i)	*mm*	1/2	0	0.2525(2)	0.38(5)
Sn_1	2(e)	6*mm*	0	0	0.1624(1)	0.41(4)
Sn_2	2(d)	$\bar{6}2m$	1/3	2/3	1/2	0.33(8)
Sn_3	2(c)	$\bar{6}2m$	1/3	2/3	0	0.43(6)

(*I*4/*mmm*) type structures [2–4]. Single-crystal experiments [5] clearly confirmed that our samples belong to the $HfFe_6Ge_6$-type structure and possible mixing between manganese, rare earth and tin atoms is totally excluded. The atomic positions of $TbMn_6Sn_6$ and the lattice parameters of all the samples are given in Tables 1 and 2. They allow us to calculate the main interatomic distances between magnetic atoms (Table 3, Fig. 1).

4. Neutron diffraction

Neutron diffraction experiments were carried out at the Institut Laue-Langevin, Grenoble. The diffraction patterns were recorded with the one-dimensionally curved multidetector D1b at the wavelength $\lambda = 2.5293$ Å. In each case, several patterns were collected in the temperature range 2–300

TABLE 2

Lattice parameters of RMn_6Sn_6 compounds (R≡Tb, Ho) and $TbCo_5$ (space group, *P6/mmm*)

Compound	a (Å)	c (Å)	V (Å^3)	Reference
$TbMn_6Sn_6$	5.530(1)	9.023(2)	238.9	[5]
$HoMn_6Sn_6$	5.505(4)	8.991(8)	236	This study
$TbCo_5$	4.950	3.979	84.4	[4]

TABLE 3

Main interatomic distances between magnetic atoms in $TbMn_6Sn_6$ (the distances d_i are related to those indicated on Fig. 1)

	Atom to atom	Type	d_i (Å)
d_1	Mn–Mn	In plane	2.7650(4)
d_2	Tb–Mn	Interplane	3.554(1)
d_3	Mn–Mn	Interplane	4.556(2)
d_4	Mn–Mn	Interplane	4.466(2)
d_5	Tb–Tb	In plane	5.530(1)
d_6	Tb–Mn	Interplane	7.331(4)

K. No pattern was collected in the paramagnetic state ($T_C > 300$ K). Using the Fermi length of ref. 6 and the magnetic form factor of manganese and R^{3+} ions of ref. 7, the scaling factor, the atomic positions z_{Mn} and z_{Sn1} (Table 1) and the magnetic moment of manganese and R^{3+} were refined by using a least-squares procedure [8]. The MXD program allows us to fit the nuclear and magnetic intensities simultaneously to the observed quantities.

4.1. $TbMn_6Sn_6$

The neutron diffraction patterns collected from 300 to 2 K only reveal an increase in the intensities of the nuclear reflections which indicates the occurrence of ferromagnetic ordering of both manganese and terbium sublattices (Fig. 2). Below 300 K, the absence of magnetic contributions to the (00*l*) reflections indicates that the moments are aligned along the *c* axis. In agreement with the magnetic measurements [2], the best refinement leads us to retain unambiguously a collinear ferrimagnetic arrangement due to an antiferromagnetic coupling between terbium and manganese ferromagnetic sublattices (Fig. 3). The values of the magnetic moments and the *z* atomic positions obtained at 250 and 2 K as well as the observed and calculated intensities are presented in Table 4.

At 300 K, the intensity of the (001) reflection is found to be non-zero (also shown in Fig. 2). This clearly indicates that a magnetic component perpendicular to the *c* axis arises at this temperature, on either terbium or manganese sites or on both. Using the low temperature magnetic structure previously defined with ϕ (the deviation from the [001] direction) as an

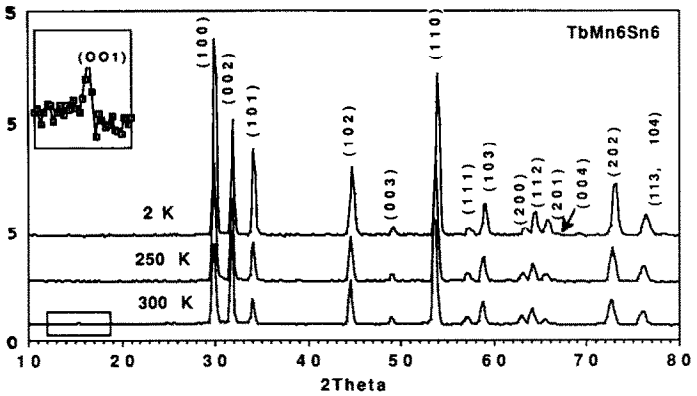

Fig. 2. Neutron diffraction patterns of $TbMn_6Sn_6$ at 300, 250 and 2 K.

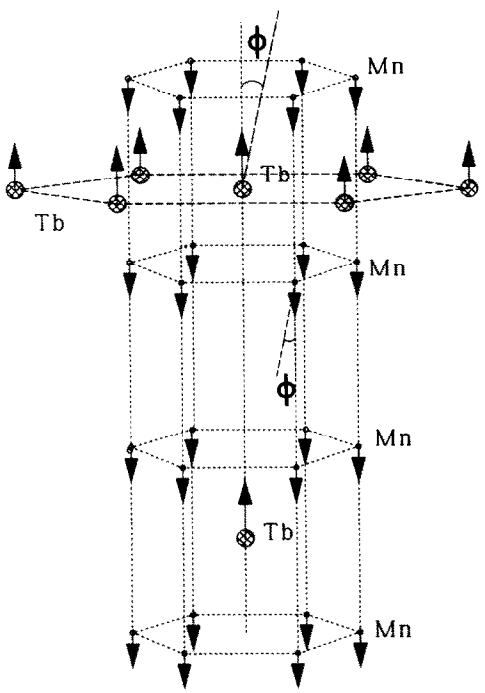

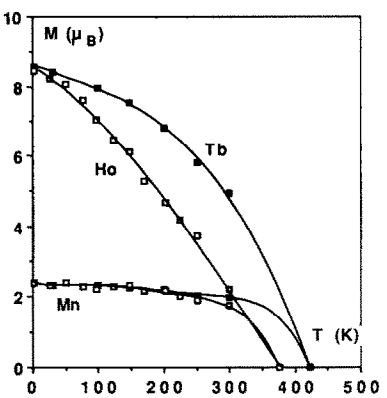

Fig. 3. Magnetic structure of $TbMn_6Sn_6$ at 2 K (ϕ is the deviation angle at high temperature; see text).

Fig. 4. Temperature dependence of the terbium, holmium and manganese magnetic moments in RMn_6Sn_6 compounds (R≡Tb, Ho).

additional parameter, the best fit to the data leads to a canting angle (on both terbium and manganese sublattices) of about 15° at 300 K (Table 4, Fig. 3). These results are in fair agreement with the pseudo-single-crystal magnetic measurements [2]. Nevertheless, in order to determine precisely

TABLE 4

Observed and calculated intensities, atomic positions z, magnetic moments, deviation angle ϕ from the c axis and reliability factors at 300, 250 and 2 K for $TbMn_6Sn_6$

hkl	$T=300$ K		$T=250$ K		$T=2$ K	
	I_c	I_o	I_c	I_o	I_c	I_o
001	4	4(1)	1	0(1)	1	0(1)
100	836	840(3)	937	961(9)	1475	1474(3)
002	961	970(3)	873	853(6)	805	843(3)
101	301	310(7)	398	418(9)	803	899(3)
102	858	870(5)	832	813(9)	989	1109(6)
003	189	158(3)	175	148(7)	138	148(3)
110	3627	3617(9)	3557	3499(19)	3877	3869(8)
111	280	278(5)	375	375(16)	760	759(7)
103	949	890(6)	922	862(13)	1059	1005(7)
200	388	394(9)	336	344(13)	293	325(7)
112	818	836(9)	808	799(16)	803	883(8)
201	218	245(10)	301	367(13)	700	728(8)
004	9	–	6	–	16	–
202	1830	1813(16)	1969	2124(46)	2995	2954(16)
104,113	1144	1173(18)	1129	1221(24)	1418	1407(18)
z_{Mn}	0.254(1)		0.254(2)		0.250(2)	
z_{Sn1}	0.168(1)		0.168(2)		0.177(4)	
μ_{Mn}/μ_B	1.99(6)		2.01(9)		2.39(8)	
μ_{Tb}/μ_B	4.95(12)		5.82(11)		8.57(12)	
ϕ (°)	15(2)		0		0	
R (%)	1.8		4.5		3.0	

the rotation phenomenon of the easy axis ($T_t=330$ K) in $TbMn_6Sn_6$, neutron diffraction studies above 300 K are in progress.

The thermal variations in terbium and manganese magnetic moments are shown in Fig. 4. They clearly indicate that both the terbium and the manganese sublattices order simultaneously at $T_C=423$ K ($\mu_{Tb}=4.95(12)\mu_B$ at 300 K).

4.2. $HoMn_6Sn_6$

Several neutron diffraction patterns have been recorded from 300 to 2 K (Fig. 5). They are quite similar to those observed for $TbMn_6Sn_6$ yielding the same ferromagnetic ordering onto the holmium and manganese sublattices. However, the intensity of the (001) reflection is always non-zero, indicating a magnetic component perpendicular to the c axis in the whole temperature range. On the basis of the collinear high temperature magnetic structure previously defined for $TbMn_6Sn_6$, the best fits to the data give canting angles of about 49° and 90° at 2 K and 300 K respectively (Table 5, Fig. 6). As observed in $TbMn_6Sn_6$, a spin reorientation (SR) process occurs in $HoMn_6Sn_6$.

In order to check this SR, we have followed the thermal dependence of the intensities of the (001) and (101) reflections. They are almost of

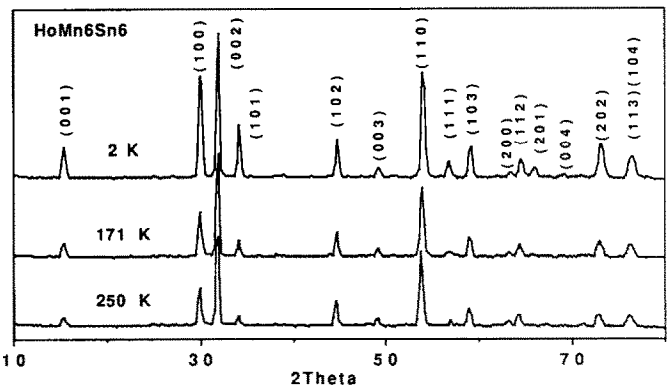

Fig. 5. Neutron diffraction patterns of $HoMn_6Sn_6$ at 250, 171 and 2 K.

TABLE 5

Observed and calculated intensities, atomic positions z, magnetic moments, deviation angle ϕ from the c axis and reliability factors at 250, 171 and 2 K for $HoMn_6Sn_6$

hkl	$T=250$ K		$T=171$ K		$T=2$ K	
	I_c	I_o	I_c	I_o	I_c	I_o
001	15	15(1)	47	48(1)	79	81(1)
100	176	177(3)	482	482(3)	937	937(3)
002	489	480(5)	1228	1237(4)	1250	1255(4)
101	65	65(3)	210	210(3)	578	581(3)
102	234	232(7)	574	586(6)	684	697(6)
003	82	77(7)	208	201(6)	231	222(5)
110	1036	1014(14)	2609	2651(13)	3052	3089(11)
111	50	43(8)	156	156(7)	482	475(7)
103	333	323(10)	870	829(9)	1099	1045(8)
200	95	78(10)	226	243(9)	203	236(8)
112	247	244(12)	604	682(12)	782	815(11)
201	35	25(9)	114	132(10)	395	449(10)
004	22	4(21)	42	18(11)	16	–
202	480	466(21)	1298	1361(19)	2229	2300(21)
104,113	477	459(18)	1264	1243(18)	1679	1755(30)
z_{Mn}	0.255(1)		0.255(1)		0.254(1)	
z_{Sn1}	0.172(1)		0.171(2)		0.169(3)	
μ_{Mn}/μ_B	2.18(7)		2.18(6)		2.39(7)	
μ_{Ho}/μ_B	4.68(12)		5.27(9)		8.43(11)	
ϕ (°)	90		76(3)		49(1)	
R (%)	3.2		2.8		3.0	

purely magnetic origin (*i.e* very weak nuclear contributions) and essentially depend on thermal variations of both parameters ϕ and μ_{Ho}. Thus, the ratio of their intensities is only correlated with ϕ. The thermal behaviour of this ratio (Fig. 7(a)) shows clearly that the rotation of the magnetic moments from the (001) plane is a continuous process between 125 and 175 K while,

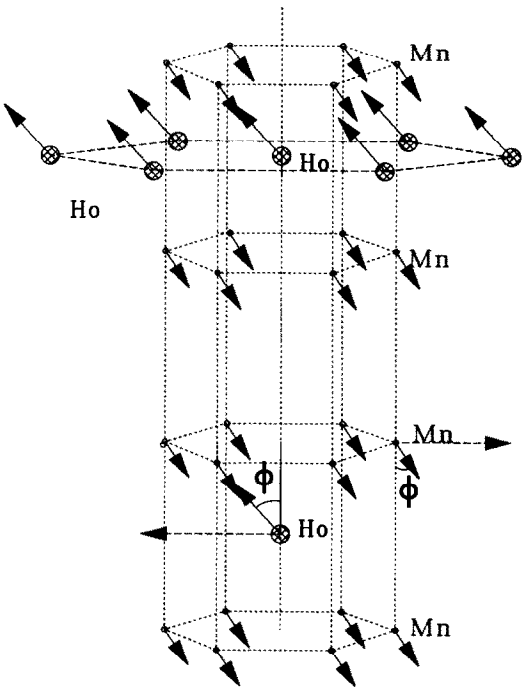

Fig. 6. Magnetic structure of $HoMn_6Sn_6$ at 2 K (ϕ is the deviation angle at high temperature; see text).

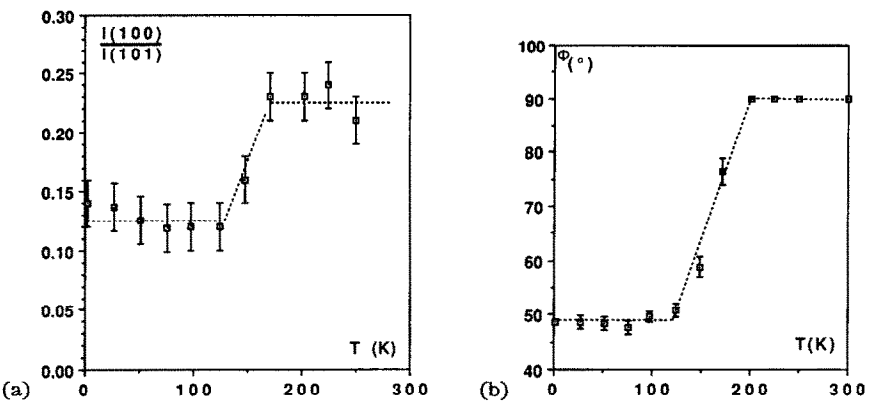

Fig. 7. Temperature dependence in $HoMn_6Sn_6$ of (a) the ratio of the intensities of the (100) and (101) reflections and (b) the canting angle ϕ (see Fig. 6).

above and below this temperature range, the moments are in the basal plane and at about 50° from the c axis respectively (Fig. 7(b)). Table 5 gives the calculated and observed intensities at 2, 171 and 250 K as well as the different adjustable parameters (z, ϕ, μ_{Mn}, μ_{Ho}). The anomaly in susceptibility, observed above 200 K in the magnetic measurements, corresponds well to this rotation of the easy axis.

The thermal variations in the magnetic moments of holmium and manganese atoms are shown in Fig. 4. As observed in $TbMn_6Sn_6$, these data show that both the holmium and the manganese sublattices order simultaneously at $T_C = 376$ K ($\mu_{Ho} = 4.68(12)\mu_B$ at 250 K).

5. Discussion

In this paper, a neutron diffraction study of the magnetic properties of the RMn_6Sn_6 (R ≡ Tb, Ho) compounds is reported.

First we remark on the Mn–Mn interactions. In the (001) manganese planes (d_1, K layer, Fig. 1), they are always ferromagnetic and probably strong, in agreement with the Slater–Néel curve, and the experimental Curie temperatures [2]. According to the neutron diffraction investigations, the saturated manganese magnetic moments have nearly the same values (about $2.2\mu_B$) in the two compounds and exhibit a classical thermal behaviour (Fig. 4). Moreover, it may be noted that these values are close to those observed in various binary and ternary intermetallic manganese compounds (such as $MnSn_2$ and $RMn_2Si(Ge)_2$ and $RMnSi_2$) [9–11]. On the contrary, the sign of the Mn–Mn interlayer exchange coupling appears to be very sensitive to the rare earth element.

As generally observed in rare earth–3d intermetallics, the R–Mn couplings are negative in both $TbMn_6Sn_6$ and $HoMn_6Sn_6$ compounds. This exchange interaction is very strong causing the rare earth moments to order simultaneously with the manganese moments. The resulting magnetic structures could be easily explained in terms of exchange couplings if we assume either negative R–Mn interactions between nearest neighbours and positive Mn–Mn interactions between adjacent manganese layers (d_3) or negative R–Mn interactions between nearest and next-nearest neighbours (d_2 and d_6 (Fig. 1 and Table 3).

On the contrary, it is found that, in RMn_6Sn_6 compounds, the magnetic easy axis direction exhibits a strong dependence on the rare earth element. For $LuMn_6Sn_6$ (*i.e.* non-magnetic rare earth) [12], an easy plane prevails throughout the temperature range 2–300 K while holmium and terbium exhibit a change in the easy direction over some part of the temperature range studied. For $HoMn_6Sn_6$, the manganese and holmium moments lie in the basal plane down to $T_{SR} = 200$ K and rotate to the c axis at lower temperature. For $TbMn_6Sn_6$, the easy c axis prevails even almost up to room temperature. The rare earth contribution to the magnetic anisotropy in RCo_5 compounds leads to the opposite behaviour: at low temperature, the $\alpha_j < 0$ type compounds (*e.g.* terbium and holmium) exhibit an easy plane character [13]. Comparison between the two series seems interesting since the local symmetries of the rare earths are the same (*P6/mmm*) and the coordination polyhedra are very similar (Fig. 1). However, a significant difference comes from the axial bonding of a rare earth with two rare earth atoms at $d \approx 4$ Å in RCo_5

compounds instead of two tin atoms at $d \approx 3$ Å in RMn_6Sn_6 compounds. The out-of-axis bondings are similar in atoms (R → R and Co → Mn) and in distances (Fig. 1).

According to Greedan and Rao [14], the rare earth sublattice orientation is determined by the sign of

$$B_2^0 = \alpha_j \langle r^2 \rangle (1 - \sigma_2) K_2^0 A_2^0$$

which depends simultaneously on α_j and A_2^0. Since the Stevens factor α_j depends only on the nature of the rare earth atoms, the determining factor is A_2^0. This is determined by the electrostatic potential due to the environment, and is given in the point charge approximation by [15]

$$A_2^0 = (-1)^{+1} \frac{4\pi}{5} e^2 \sum_k \frac{Z_k}{R_k^3} Y_2^0(\theta_k)$$

where Z_k and R_k are respectively the charge and the distance to the kth ion in the environment of the reference rare earth atom.

Following Greedan and Rao [14], a [001] easy axis direction indicates that B_2^0 should be negative. Assuming a negative effective charge associated with the axial Sn(1) atom in RMn_6Sn_6 yields $A_2^0 > 0$ (contrary to tripositive rare earth ions in RCo_5 [15] and $A_2^0 < 0$), we consider that the low temperature axial behaviour of $TbMn_6Sn_6$ and $HoMn_6Sn_6$ is due to the effective charge Z_k of Sn(1), which effect is reinforced by the short R–Sn(1) distance R_k.

Then it seems clear that, in RMn_6Sn_6 compounds, the magnetocrystalline anisotropy is determined by competing contributions from the manganese and the rare earth sublattices. The manganese sublattice favours an easy plane behaviour ($LuMn_6Sn_6$). It is also observed in closely related FeSn and Fe_3Sn_2 binary stannides [16]. At low temperature, the rare earth sublattice favours an easy axis for both holmium and terbium. It should be noted that the uniaxial magnetocrystalline anisotropy is much larger for terbium than for holmium since in $HoMn_6Sn_6$ the reorientation process is not achieved ($\phi \approx 50°$) at low temperature. These behaviours should be related to the different coercive properties observed between these two compounds.

The last remark concerns the magnitude of the rare earth magnetic moments and their unusual thermal variations (Fig. 4). The values deduced from neutron diffraction experiments are close to the free ion values or are slightly reduced (about 15%) with respect to the free ion values in $TbMn_6Sn_6$ and $HoMn_6Sn_6$. A similar thermal variation has been observed in the RFe_6Al_6 compounds isotypic with $ThMn_{12}$ [17]. For instance, in $DyFe_6Al_6$, Mössbauer spectroscopy shows that the thermal variation in the reduced ^{161}Dy hyperfine fields exhibits a similar behaviour. This unusual variation can be regarded as resulting from two Brillouin curves: the low temperature part could be related to the "intrinsic" rare earth moment ordering and the high temperature part to the polarization of the rare earth moment by the transition metal sublattice. This transition does not appear in the magnetic experiments, but it could be detected by specific heat and resistivity measurements. Furthermore, it may be noted that this peculiar behaviour is less pronounced in $TbMn_6Sn_6$

than in $HoMn_6Sn_6$ which displays the smaller uniaxial anisotropy and a reduced moment.

6. Conclusion

The neutron diffraction experimental results lead us to the following conclusions:

(1) RMn_6Sn_6 compounds order at relatively high temperature owing to strong ferromagnetic Mn–Mn intrasublattice exchange.

(2) A strong antiferromagnetic Mn–R coupling causes the rare earth sublattice to order simultaneously with the manganese sublattice. It constrains the rare earth moments to be collinear with the manganese moments. This behaviour yields collinear ferrimagnetic arrangements for both compounds in the entire temperature range.

(3) Analysis of the magnetic ordering of RMn_6Sn_6 (R≡Tb, Ho, Y) compounds provides information about the magnetic anisotropy and exchange interactions in this series. In $TbMn_6Sn_6$ and $HoMn_6Sn_6$ the exchange interactions between rare earth and manganese atoms have a significant influence on the magnetic properties. The stability of the collinear magnetic structures ((001) ferromagnetic planes) may be ascribed either to anisotropic exchange interactions arising from orbital polarization of the conduction electrons or to rare earth–single ion anisotropy plus exchange interactions. In $TbMn_6Sn_6$, the reorientation of the rare earth moments with respect to the [001] axis is probably determined by the second-order crystal field term B_2^0. Following Greedan and Rao [14], a [001] easy axis direction indicates that B_2^0 should be negative. In $TbMn_6Sn_6$, the rare earth uniaxial anisotropy is apparently dominant, even at room temperature, while in $HoMn_6Sn_6$ the magnetic configurations depend not only on the rare earth ion but also on the transition metal element and this compound exhibits an easy plane (as in $LuMn_6Sn_6$) above 200 K. Nevertheless, the influence of crystal field effects may probably explain the partial quenching of the rare earth moment which is somewhat smaller than the rare earth free ion value in $HoMn_6Sn_6$.

These studies are to be completed by magnetic measurements on oriented samples in order to determine quantitative values for anisotropy and exchange. Furthermore, in order to determine precisely the SR direction in $TbMn_6Sn_6$, neutron diffraction investigations in the temperature range from 300 K to T_N (T_C) are required. In order to check the magnetic structures of $DyMn_6Sn_6$, $ErMn_6Sn_6$ and $TmMn_6Sn_6$, investigations by neutron diffraction and rare earth Mössbauer spectroscopy measurements are in progress.

Acknowledgments

Neutron diffraction data were recorded at the Institut Laue Langevin. We are grateful to J. L. Soubeyroux, responsible for the D1b spectrometer and for his help during the measurements.

References

1 B. Malaman, G. Venturini and B. Roques, *Mater. Res. Bull., 23* (1988) 1629.
2 G. Venturini, B. Chafik El Idrissi and B. Malaman, *J. Magn. Magn. Mater., 94* (1991) 349.
3 R. R. Olenitch, L. G. Akselrud and Ya. P. Yarmoliuk, *Dopov. Akad. Nauk Ukr. R.S.R., Ser. A,* (2) (1981) 84.
4 P. Villars and L. D. Calvert, *Pearson's Handbook of Crystallographic Data for Intermetallic Phases*, American Society for Metals, Metals Park, OH, 1985.
5 B. Chafik El Idrissi, G. Venturini and B. Malaman, *Mater. Res. Bull.*, to be published.
6 A. J. Freeman and J. P. Declaux, *J. Magn. Magn. Mater., 12* (1979) 11.
7 C. Stassis, H. W. Deckmann, B. N. Harmon, J. P. Desclaux and A. J. Freeman, *Phys. Rev. B 15* (1977) 369.
8 P. Wolfers, *J. Appl. Cryst., 23* (1990) 554.
9 G. Le Caer, B. Malaman, G. Venturini and I. B. Kim, *Phys. Rev. B, 26*(9) (1982) 2009.
10 A. Szytula and J. Leciejewicz, K. A. Gschneidner, Jr. and L. Eyring (eds.) *Handbook on the Physics and Chemistry of Rare Earths*, Vol. 12, Elsevier, Amsterdam, 1989, p. 133.
11 B. Malaman, G. Venturini, L. Pontonnier and D. Fruchart, *J. Magn. Magn. Mater., 86* (1990) 349.
12 G. Venturini, B. Chafik El Idrissi, D. Fruchart and B. Malaman, to be published.
13 R. Lemaire, *Cobalt, 32* (1966) 132.
14 J. E. Greedan and C. N. Rao, *J. Solid State Chem., 6* (1973) 387.
15 W. E. Wallace, *Rare Earth Intermetallics*, Academic Press, New York, 1973, Chap. 3.
16 B. Malaman, G. Le Caer and D. Fruchart, *J. Phys. F, 8* (11) (1978) 2389.
17 I. Felner, M. Seh, M. Rakavy and I. Nowick, *J. Phys. Chem. Solids, 42* (1981) 369.